OPEN ACCESS
IOP Publishing
Journal of Physics A: Mathematical and Theoretical
J. Phys. A: Math. Theor. **53** (2020) 345703 (14pp)
https://doi.org/10.1088/1751-8121/ab9da3

Dispersive focusing in fractional Korteweg–de Vries-type equations

Elena Tobisch[1,4] **and Efim Pelinovsky**[2,3]

[1] Institute for Analysis, Johannes Kepler University, Linz, Austria
[2] National Research University-Higher School of Economics, Moscow, Russia
[3] Russian Academy of Sciences, Institute of Applied Physics, Nizhny Novgorod, Russia

E-mail: elena.tobisch@jku.at

Received 21 February 2020, revised 5 June 2020
Accepted for publication 17 June 2020
Published 3 August 2020

Abstract

In this paper we study dispersive enhancement of a wave train in systems described by the fractional Korteweg–de Vries-type equations of the form $u_t + \alpha_n u^n u_x + \beta_m (D_m\{u\})_x = 0, D_m\{u\} = -|k|^m u(k)$ where the operator $D_m\{u\}$ is written in the Fourier space, α_n, β_m are arbitrary constants and n, m being rational numbers (positive or negative). Using both approximate and exact solutions of these wave equations we describe constructively the process of dispersive focusing. It is based on a time-reversing approach with the expected rogue wave chosen as the initial condition for a solution of these equations. We demonstrate the qualitative difference in the shape of the focused wavetrains for various n and m. Our results can be used for prediction of the rogue wave appearance arising in many types of weakly nonlinear and weakly dispersive wave systems in physical context.

Keywords: Korteweg–de Vries equation, nonlinear waves, dispersive focusing, rogue waves

(Some figures may appear in colour only in the online journal)

1. Introduction

Dispersion enhancement of wave packets is one of the main mechanisms for generating abnormally large waves called rogue waves. The idea of this mechanism is quite straightforward: in a dispersive medium, the group velocity depends on the frequency, and wave packets with

[4] Author to whom any correspondence should be addressed.

different wavelengths can either diverge or converge in space. Profound theoretical studies of this mechanism have been presented in [1–5]. The feasibility of this mechanism has been observed recently in the oceanic data, [6].

Dispersion enhancement is one of a few quasi-linear mechanisms of the wave focusing, together with e.g. geometrical focusing, and their features can be studied in the frame of linear PDEs. It is important to realize that nonlinearity not necessarily prevents dispersive enhancement of wave packets, although, of course, it affects the characteristics of the resulting rogue waves. This mechanism is very often used in water wave tanks for generating rogue waves, see for instance [1].

In this paper we study the family of the Korteweg–de Vries (KdV) equations with fractional derivatives

$$u_t + \alpha_n u^n u_x + \beta_m (D_m\{u\})_x = 0, \tag{1}$$

$$\text{with } D_m\{u\} = -|k|^m u(k), \tag{2}$$

$$u(k,t) = \int_{-\infty}^{+\infty} u(x,t) \exp\{\mathrm{i}kx\}\, \mathrm{d}x, \tag{3}$$

n, m are rational numbers (positive or negative), and α_n, β_m are arbitrary constants, and for simplicity of presentation we assume them positive. Equations of the form (1) appear in numerous applied problems of fluid dynamics, plasma physics, etc. Not to give an extensive review, we recall just a few most famous examples of the equations belonging to this family. Completely integrable equations of this type are given, for instance, by the classical KdV equation ($m = 2, n = 1$), modified KdV equation ($m = 2, n = 2$), integral Benjamin–Ono equation ($m = 1, n = 1$), [7]. We would like to mention that many non-intergable equations belonging to this class, such as classical ($m = 4, n = 1$) and modified ($m = 4, n = 2$) Kawahara equations, [8–10]; Shamel equation ($m = 2, n = 1/2$), [11]; $(2 + 4)$-KdV equation ($m = 2, n = 4$), [13]; reduced Whitham equation for short gravity waves ($m = 1/2$, $n = 1$), [12]; reduced Ostrovsky equation ($m = -2$, $n = 1$ or 2), [14]. In addition, some studies are available where the equation (1) is regarded with negative nonlinearities, e.g. [15], however, these cases will not be analyzed here.

In this paper we aim to present a constructive study of general characteristics of the dispersive focusing of wave trains into the rogue wave in the media described by the equations (1)–(3) using their exact and approximate solutions.

2. Evolution equations and dispersion characteristic

In the approximation of linear long waves of many types propagating in one direction, the dispersion characteristic is approximated by the first two terms

$$\omega = ck - \beta_m |k|^m k \tag{4}$$

where k is the wave number, ω is its frequency, c is the speed of linear long waves, and β_m is a numerical coefficient, the dimension of which can be found from equation the equation (4). The exponent is assumed to be non-zero (otherwise the medium does not have dispersion), and it can be both positive and negative. The sign of the module k in the equation (4) is included to consider wave numbers and frequencies in the negative range, which is convenient for a comprehensive Fourier analysis of wave processes. Methods which allow to construct a

linear, nonlinear or even integro-differential evolution equations with given dispersion functions are presented and studied in detail in the classical monograph [12]. In particular, from the dispersion equation (4) we can pass to the evolution equation

$$\frac{\partial u}{\partial t} + c\frac{\partial u}{\partial x} + \beta_m \frac{\partial}{\partial x} D_m\{u\} = 0, \tag{5}$$

where the operator $D\{u\}$ has the following Fourier presentation:

$$D_m\{u\} = -|k|^m u(k). \tag{6}$$

Here $u(k)$ is a spatial Fourier spectrum (in general case, it is complex),

$$u(k) = \int_{-\infty}^{+\infty} u(x,t) \exp(\mathrm{i}kx)\, \mathrm{d}x. \tag{7}$$

Finally, it is important to emphasize that it is possible to switch to a frame of reference moving with the speed of linear long waves, so that without loss of generality we put $c = 0$. This is the standard form for studying dispersive waves in the frame of fractional KdV-type equations, see e.g. [16] and bibliography therein.

Accordingly, below we firstly regard the equations (1)–(3) with $\alpha_n = 0$. The resulting linear equation

$$u_t + \beta_m (D_m\{u\})_x = 0 \tag{8}$$

has a general solution which can be presented by the corresponding Fourier integral as

$$u(x,t) = \frac{1}{2\pi} \int_{-\infty}^{+\infty} u(k) \exp\{\mathrm{i}[\omega(k)t - kx]\} \mathrm{d}k, \tag{9}$$

where $u(k)$ is the spectrum of the initial excitation, $u(k) =_u^* (k)$ (this condition provides that spectrum $u(k)$ is real) and the wave frequency is described by the dispersion functions as

$$\omega(k) = -\beta_m |k|^m k. \tag{10}$$

Our goal is to study the process of dispersive focusing of wave packets, which in the framework of the linear problem is reduced to solving the equation (8) with previously unknown initial conditions, because only some of them will lead to the formation of large waves. One can use the invert property of the equation (8) with respect to the sign of time and coordinate, set the initial condition in the form of the expected rogue wave, and see how it turns into a wave packet of small amplitude. By inverting the obtained solution then, we can be sure of its transformation into a rogue wave of a given shape. This method, called time-reversing, was applied in [17] for the analysis of rogue waves in the framework of the KdV equation, and later in [18, 19] for the nonlinear Schrödinger equation.

3. Approximate description of the dispersive focusing

The simplest way to study the effects of dispersive focusing of frequency-modulated wave packets is to regard the framework of the Whitham's kinematic equation for the local value of

the wave number $k(x, t)$ and wave amplitude $A(x, t)$, [12]. For definiteness, only positive values of the wave numbers are considered here:

$$\frac{\partial k}{\partial t} + c_{\rm gr}(k)\frac{\partial k}{\partial x} = 0, \tag{11}$$

$$\frac{\partial A}{\partial t} + \frac{\partial}{\partial x}(c_{\rm gr}A) = 0 \tag{12}$$

where the group velocity of the wave packet can be found from the dispersion relation given ba the equation (10) as follows:

$$c_{\rm gr} = \frac{{\rm d}\omega}{{\rm d}k} = -(m+1)\beta_m k^m. \tag{13}$$

It is easy to demonstrate, [1], that optimal process of focusing of the wave packets is described by the self-similar solution

$$c_{\rm gr} = \frac{x_f - x}{t_f - t}, \tag{14}$$

$$A = A_0\sqrt{\frac{t_f}{t_f - t}}, \tag{15}$$

where A_0 is initial magnitude of the amplitude, x_f is the space coordinate and t_f is the moment of time describing when and where all wave packets will be gathered in one place at the same time. It follows from the equation (14) that the initial distribution of the wave number in the train has the form

$$k(x, 0) = \left[\frac{x - x_f}{(m+1)\beta_m t_f}\right]^{1/m}. \tag{16}$$

and it can be seen from the equation (15) that the wave amplitude tends to infinity when approaching the focal point. This physically demonstrative solution, however, does not work in the vicinity of the focus and does not allow predicting the shape of the emerging rogue wave.

4. Self-similar solutions and an 'ideal' rogue wave

Obviously, the ideal presentation of a rogue wave in linear theory is delta-function. Indeed, the main characteristics of a rogue wave are big amplitude, big steepness and short living times compare to other excited waves in the wavefield. The simplest relevant parameter allowing to characterize rogue wave is the ratio of its height $H_{\rm rogue}$ to the significant wave height $H_{\rm s}$ which is the average wave height among one third of the highest waves in a time series (usually of length of 10 to 30 min), [1]. For rogue wave, condition $H_{\rm rogue}/H_{\rm s} > 2$ should be satisfied. In various physical contexts, additional demand for the relation between $H_{\rm rogue}$ and wave steepness may be written out. Thus, speaking very generally, difference between rogue and all other waves is just *quantitative*. On the other hand, delta function has infinite height and infinite steepness as defined by its derivative, that is, it differs *qualitatively* from other waves in the field. Accordingly, delta-function can be regarded as an ideal, limiting case of a 'physical' rogue wave and precisely in this sense we use the phrasing 'ideal' rogue wave below. The study of this limiting case proved to give useful insight for further exploration of physical rogue waves.

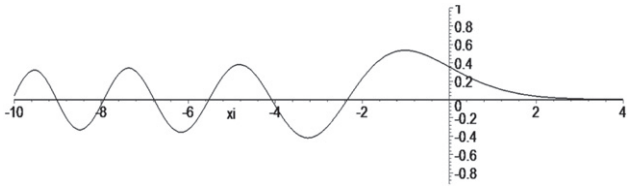

Figure 1. Airy function, self-similar solution for $m = 2$ (the linearized Korteweg–de Vries equation).

Let write out corresponding solution for the equation (9) assuming the initial excitation in the form of delta-function

$$u_0(x) = A_0\,\delta\left(\frac{x}{l}\right), \tag{17}$$

so that $u_0(k) = A_0 l$ and the wave field is described by the integral

$$u(x,t) = \frac{A_0 l}{\pi}\int_0^{+\infty} \cos[\omega(k)t - kx]\mathrm{d}k. \tag{18}$$

This integral can be rewritten in a form more suitable for further analyzing, namely,

$$u(x,t) = \frac{A_0 l}{2\sqrt[m+1]{3\beta_m t}}\Phi\left[\frac{x\,\beta_m}{\sqrt[m+1]{3\beta_m t}}\right], \tag{19}$$

$$\Phi(\xi) = \frac{1}{\pi}\int_0^{\infty} \cos\left[\xi z + \frac{z^{m+1}}{3}\right]\mathrm{d}z. \tag{20}$$

Now we can see that solution $u(x,t)$ given by the equations (19) and (20) is self-similar while the spatial distribution of the dependent variables remains similar during all time evolution. The crucial role of self-similar solutions in the study of nonlinear waves is due to the fact that 'they describe the 'intermediate asymptotic' behavior of solutions of wider classes of initial, boundary, and mixed problems', [21].

It is important to understand that due to the dispersion, an arbitrary initial excitation turns into a wave train at the big times. Indeed, in dispersive system the group speed depends on the wave vectors, i.e. all Fourier modes of the initial excitations propagate at different speeds and, after suitably long time, a narrow initial excitation turns into a train containing multitude of waves, with different amplitudes. The first wave in this train is called leading wave and it has maximal group speed. Below we demonstrate that the time evolution of the wave field depends on whether or not the leading wave has also the maximal amplitude.

Let us notice straightaway that for $m = 2$, the equation (8) reduces to the linearized KdV equation, and the function $\Phi(\xi)$ is expressed in terms of the known Airy function of the first kind, [23],

$$\Phi(\xi) = \mathrm{Ai}(\xi) \tag{21}$$

shown in the figure 1. As a result, the wave field given by the equation (19) describes a train decaying with time as $t^{-1/3}$ and its maximal leading wave that spreads out in space proportionally to $t^{1/3}$. This process is well known for the linear Korteweg–de Vries equation, [7, 12].

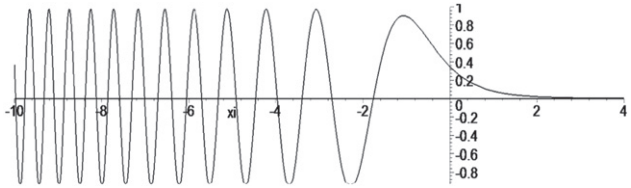

Figure 2. Self-similar solution for $m = 1$ (the linearized Benjamin–Ono equation).

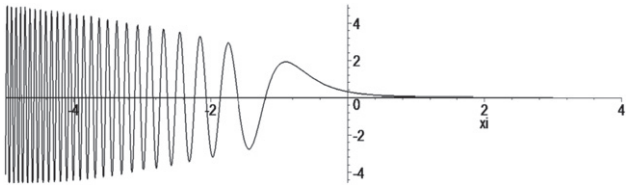

Figure 3. Self-similar solution for $m = 1/2$.

In the case when $m = 1$, the equation (19) is reduced to the linearized Benjamin–Ono equation, and the function $\Phi(\xi)$ is also expressed in terms of special functions (first obtained in [22])

$$\Phi(\xi) = \sqrt{\frac{6}{\pi}} \left\{ \sin\left(\frac{3\xi^2}{4}\right) \left[1 - 2S\left(\sqrt{\frac{3}{2\pi}}\xi\right)\right] + \cos\left(\frac{3\xi^2}{4}\right) \left[1 - 2C\left(\sqrt{\frac{3}{2\pi}}\xi\right)\right] \right\}, \quad (22)$$

where $S(\xi)$ and $C(\xi)$ are the Fresnel integrals, [23]. This function is shown in the figure 2, and we observe that in this case the wave field behind the leading wave does not decay but the leading wave decreases with time as $t^{-1/2}$, and spreads in space as as $t^{1/2}$.

For $m = 1/2$, a self-similar solution explicitly expressed in terms of special functions can also be obtained by a suitable program packets for symbolical computations, e.g. Maple or Mathematica. This expression is rather cumbersome and is not given here. However, its shape is shown in the figure 3. In this case the wave field grows unboundedly with growing distance from the leading wave.

In general case, however, it is not possible to analytically calculate the integral given be the equation (20) and reduce the function to the known ones. Therefore, it is not clear how many different characteristics of self-similar solutions obtained are inherent in media with an arbitrary value of m. In order to gain more understanding, we study the asymptotic of the self-similar solution given by the equations (19) and (20) at large times in the region $x < 0$ using the stationary phase method, [7, 12]. The wave field can be represented as follows, [24]:

$$u(k, t) = A(x, k_*; t) \cos\left[\Psi(x, k_*; t)\right] \quad (23)$$

where

$$c_{\mathrm{gr}}(k_*) = \frac{\mathrm{d}\omega}{\mathrm{d}k} = -(m+1)\beta_m k_*^m = \frac{x}{t}. \quad (24)$$

The envelope of the wave packet now has the form

$$A(x,t) = A_0 l \sqrt{\frac{2}{m}} \frac{(-x)^{\frac{1-m}{2m}}}{\sqrt[2m]{(m+1)\beta_m t}} \tag{25}$$

and the phase reads

$$\Psi(x,k_*;t) = \omega(k_*)t - k_* x - \frac{\pi}{4} = -\frac{mx}{m+1}\left[\frac{-x}{\beta_m(m+1)t}\right]^{1/m} - \frac{\pi}{4}. \tag{26}$$

As expected, the amplitude of the wave decreases over time, but in space we get two qualitatively different regimes. For $m > 1$, the wave amplitude decays with moving from the leading wave located in the region near $x = 0$ (cf with the Airy function), and for $m < 1$ the wave amplitude grows unboundedly as the distance from the leading wave grows.

In the intermediate case $m = 1$, the wave amplitude is constant in space; this case has been studied in detail in [25]. The wavelength in all cases decreases with growing distance from the leading wave. Formally, solution given by the equation (24) does not work in the vicinity of the leading wave (small values of the wave number), but now we are more interested in the wave packet as a whole, rather than the first few waves, especially since for $m < 1$ they have a small amplitude compared to the amplitudes of waves behind the leading wave.

Summarizing, we have obtained the exact solution and its asymptotic presentation in the case when the initial condition is delta-function. Inverting the resulting self-similar solution in space

$$u(x,t) = \frac{A_0 l}{2\sqrt[m+1]{3|\beta_m|(t_f - t)}} \Phi\left[\frac{-x}{\sqrt[m+1]{3\beta_m(t_f - t)}}\right] \tag{27}$$

we conclude, that in the moment of time t_f the wave packet (27) will be transformed into delta-function and then spreads out again.

However, the interpretation of the obtained solution in the context of rogue waves is not unambiguous. When $m \geqslant 1$, a wave packet of small amplitude is converted into a single wave of unbounded amplitude (an ideal rogue wave). In the opposite case, the wave packet has an unbounded amplitude at one of its ends and its collapse into a delta-function does not lead to the appearance of a wave with an anomalously large amplitude. Therefore, the dispersion scenario for the formation of an ideal rogue wave does not work in this case, and it cannot arise from a low-amplitude perturbation. However, a rogue wave (but not ideal) can occur if high-amplitude tails are cut off in the wave packet. This scenario will be explored in the next section.

5. Bell-shaped rogue wave

Now consider a 'non-ideal' rogue wave given by the bell-shaped Gaussian impulse

$$u_0(x) = A_0 \ \exp\left(-\frac{x^2}{l^2}\right) \tag{28}$$

with A_0 and l being the amplitude and the half-width of the initial impulse (that is, expected freak wave) accordingly. Obviously, with $A_0 \to \infty$ and $l \to 0$, the form of this impulse turns

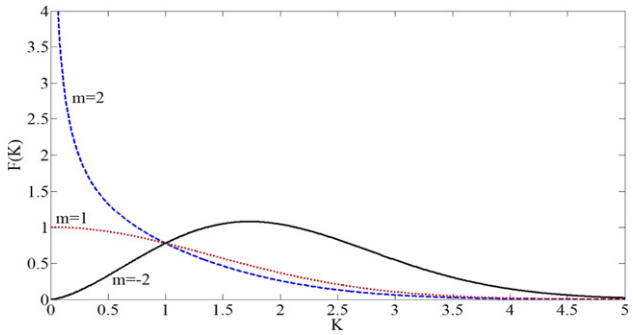

Figure 4. Spectral amplitude distribution by wave numbers in a packet.

into the delta function (an 'idea' rogue wave). However, in contrast to the delta function, in this case we have a bounded spectrum

$$u_o(k) = \sqrt{\pi} A_0 l_0 \ \exp\left(-\frac{k^2 l^2}{4}\right) \tag{29}$$

The integral (9) with this spectral function can not be calculated in a general form. However, some properties of the wave field can be determined. In the region of the leading wave (which corresponds to small wave numbers), the spectrum (29) coincides with the spectrum of the delta function, which means that the leading wave is described by the same self-similar solution as in the previous section. Far from the leading wave, we can again apply the stationary phase method, so that the wave field can be presented in the form given be the equation (23), where the amplitude takes the form

$$A(x,t,k_*(x,t)) = A_0 l \sqrt{\frac{2}{t\beta_m m(m+1)k_*^{m-1}}} \ \exp\left(-\frac{k_*^2 l^2}{4}\right) \tag{30}$$

with

$$k_* = \left[\frac{-x}{\beta_m(m+1)t}\right]^{1/m}. \tag{31}$$

The distribution of the amplitude of the wave packet depends on the type of dispersion and is defined by the function (included in expression for the amplitude)

$$F_m(K) = K^{\frac{1-m}{2}} \ \exp\left(-\frac{K^2}{4}\right), \quad K = kl \tag{32}$$

shown in the figure 4.

If $m > 1$, as in the Korteweg–de Vries and Kawahara equations, the amplitude of the first long waves is large (shown by the dashed line in the figure 4) and monotonically drops to the tail of the wave packet, where short waves are present. The wave field here differs not much from the self-similar solution described by the Airy function given in the previous section. This dynamics is well known in the framework of the linear KdV equation, [7]. In the case $m = 1$ (as in the Benjamin–Ono equation), the wave amplitude decreases with as the distance from the leading wave grows (shown by the dotted line in the figure 4), in contrast to the self-similar solution given by the equation (22).

Loosely speaking, one may think of combining these two cases together and argue that for $m \geqslant 1$ a short pulse is always converted to a train with a damping amplitude from head to tail.

A completely different dynamics arises if $m < 1$. An example is shown the figure 4 by the solid line for the reduced Ostrovsky equation. In this case, long and short waves have small amplitudes and the main energy concentrates in a wave with the wave number $k_{\max}$ and amplitude $A_{\max}$ which is moving with the constant speed $c_{\max}$:

$$A_{\max} = A_0 \sqrt{\frac{(1-m)^{\frac{1-m}{2}} l^{1+m}}{t\beta_m m(m+1)}} \exp\left(-\frac{1-m}{4}\right), \tag{33}$$

$$k_{\max} = \frac{\sqrt{1-m}}{l}, \tag{34}$$

$$c_{\max} = -\frac{\beta_m (m+1)(1-m)^{m/2}}{l^m}. \tag{35}$$

As a result, we have a wave packet with amplitude decaying with time as $t^{-1/2}$ and spreading out linearly in space (long waves go forward and short waves go back), so that its energy is conserved. The description of energy-carrying waves in this package should be conducted using the linear Schrödinger equation for the envelope in the vicinity of the wave number $k_{\max}$, [7, 12]. Thus, we have demonstrated that the initial impulse perturbation is converted into a wave packet with decreasing amplitude from the train head to its tail if $m \geqslant 1$, and into a Schrödinger-type wave packet, in which the amplitude decreases from the center of the packet in both directions if $m < 1$.

Let us now summarize the role of the obtained solutions in the context of rogue waves. By inverting solution given by the equation (23) with the amplitude (30), one can guarantee the dispersion focusing of these packets into a rogue wave of a large Gaussian shape. Differences in the dispersion laws for different media appear in the shape of focusing wave packets. For the case $m \geqslant 1$, the wave trains has gradually increasing amplitudes from head to tail (note that here the amplitude grows differently due to inversion), and for $m < 1$ the wave packet has a maximum of the wave amplitude 'in the middle' of the train.

6. Nonlinear stage of the wave field evolution

In the previous sections we examined the mechanism of dispersive focusing of wave packets into a rogue wave in the framework of linear theory. Nonlinear effects modify the evolution of wave packets. However, the time-reversing method can also be applied for studying nonlinear problems, and we can again consider the wave process as a time evolution of the expected rogue wave. Nonlinearity can be characterized by the so-called Ursell parameter, which is the ratio of the nonlinear to the dispersion term in the equation (1):

$$\mathrm{Ur} = \frac{\alpha_n}{\beta_m} A^n l^m. \tag{36}$$

Here, as before, A is the wave amplitude and l is its length. Let us assume first that the expected rogue wave is linear enough in the sense that the initial value of the Ursell parameter is small:

$$\mathrm{Ur}_0 = \frac{\alpha_n}{\beta_m} A_0^n l^m \ll 1. \tag{37}$$

Accordingly, at the first stage it is possible to solve the linear problem and the initial pulse is transformed into a wave packet which is represented by a damped train with a maximal leading

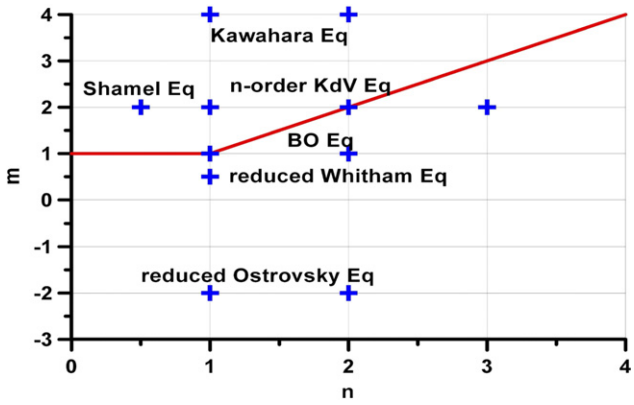

Figure 5. Schematic presentation of a few well-known PDEs given by the equation (1) on the plane of parameters m and n. Solid line corresponds to the constrains $m = 1$ and $m = n$. All equations above the solid line lead to the nonlinear regime for small initial excitation.

wave if $m \geqslant 1$ or by the Schrödinger-type packet with a maximal middle wave if $m < 1$. In the first case, the head wave is described by a self-similar solution given be the equation (19) and over time its amplitude decreases as $t^{-1/(m+1)}$, and the length grows as $t^{1/(m+1)}$. Then the local value of the Ursell parameter for the leading wave changes with time

$$\mathrm{Ur} = \frac{\alpha_n}{\beta_m} A^n(t) l^m(t) \sim t^{\frac{m-n}{m+1}}, \tag{38}$$

and grows unboundedly if $m > n$. In this case, the nonlinear effects become significant despite the fact that the wave amplitude becomes ever smaller. This fact was originally noted in [26] where, however, the leading wave limitations were not studied.

In the figure 5 the constraints $m = 1$ and $m > n$ are shown by a solid line, and all equations having m, n above this line lead to nonlinear solutions, even if the initial excitation was very small. Among these PDEs we find the classical Korteweg–de Vries equation, the Shamel equation, and the Kawahara equations with various nonlinearities. Our conclusion is in accordance with some known facts about these equations, for instance, a well-known fact is that a soliton is formed in the Korteweg–de Vries equation from an arbitrarily small positive perturbation, [7, 17]. In this context the delta-function, i.e. an 'ideal' rogue wave, has a very small initial value of the Ursell parameter and can be considered as linear.

On the other hand, for equations with m, n below the solid line, the leading wave, being linear at the beginning, remains so at any moment of time, meaning that the influence of nonlinearity on the leading wave will be small. This case is illustrated in the figure 5 by the reduced Whitham and Ostrovsky equations.

The classical Benjamin–Ono equation and the modified Korteweg–de Vries equation are special in this sense: for them the Ursell parameter remains constant. Therefore, here the leading wave remains linear at any moment in time. Due to the integrability of these equations, this property is confirmed in solving the inverse problem solitons do not arise from small initial perturbations, [27, 28].

If $m < 1$, the wave of maximal amplitude is in the 'middle' of the Schrödinger-type packet, and using the expression given by the equation (33), we find that the local Ursell parameter always decreases with time. In particular, solitons do not arise when the value of the Ursell

parameter satisfies the condition

$$\mathrm{Ur} = \frac{\alpha_n}{\beta_m} A^n(t) l^m(t) \sim t^{-\frac{n}{2}} \tag{39}$$

(which follows from [27], after suitable re-scaling) and in this sense the Ursell parameter for the expected rogue wave should be small.

Therefore, the wave packet, being linear at first, will remain linear at any moment of time. This fact is known in the theory of the integrable nonlinear Schrödinger equation—the envelope soliton can not be formed from a small perturbation, [7].

Thus, in all cases, the nonlinearity does not prevent the dispersion spreading of the initial impulse (the expected rogue wave) if its Ursell parameter is small. It is in this sense that we can speak of a quasilinear dispersion mechanism of the formation of rogue waves.

7. Discussion

In this paper we study dispersive focusing of wave train in the fractional Korteweg–de Vries-type of equations of the form

$$u_t + \alpha_n u^n u_x + \beta_m (D_m\{u\})_x = 0, \qquad D_m\{u\} = -|k|^m u(k)$$

with arbitrary constants α_n, β_m, and n, m being rational numbers (positive or negative) Essentially, two methods have been used for deriving both approximate and exact solutions of these wave equations—classical stationary phase method and comparatively new time-reversing method. The latter allows using the invert property of the equation (8) with respect to the sign of time and coordinate, set initial condition in the form of the expected rogue wave and study the process of its transformation into a wave packet of small amplitude. Our findings can be summarized as follows.

• The linear case $\alpha_n = 0$ has been analyzed in all details and the self-similar solution for this case is given explicitly by the expressions (19) and (20) depending on (generally) unknown function $\Phi(\xi)$. In some cases it can be reduced to known special functions, for instance, to the Airy function if $m = 2$ or to the expression depending on the Fresnel integrals if $m = 1$. These examples correspond to the linearized KdV and Benjamin–Ono equations consequently. We have also deduced its asymptotic presentation given by the equation (27) in the case when the initial condition is a delta-function called an 'ideal' rogue wave. We came to the conclusion that if $m \geqslant 1$, a wave packet of small amplitude is converted into a single wave of unbounded amplitude—an 'ideal' rogue wave, while for $m < 1$ no low-amplitude perturbation can generate an 'ideal' rogue wave.

An 'ideal' rogue wave is described by the delta-function, that is, by a single wave of unbounded amplitude. The natural question arises whether or not a wave of a large amplitude can occur if high-amplitude tails are cut off in the wave packet (a non-ideal rogue wave). Taking a Gaussian bell-shaped the initial impulse perturbation we have demonstrated that it is converted into a wave packet with decreasing amplitude from the train head to its tail if $m \geqslant 1$, and into a Schrödinger-type wave packet (with maximum of the wave amplitude 'in the middle' of the train), in which the amplitude decreases from the center of the packet in both directions if $m < 1$. By inverting solution given be the equation (23) with the amplitude (30), the dispersion focusing of these packets with certainty lead to the appearance of a (non-ideal) rogue wave of

a large Gaussian shape. The shape of focusing wave packets depends on the dispersion law and varies for different dispersive media.

• We have demonstrated that the role of wave packets (which, of course, are modified by nonlinearity) in the dispersive focusing mechanism is fundamental in the framework of the nonlinear problem, as it was shown before in various physical contexts, see e.g. [17–19]. Consider again the evolution of the ideal rogue wave in the form of delta-function in the framework of the original nonlinear equation (1). The exact solution to this problem is known for integrable systems. In particular, in the framework of the classical Korteweg–de Vries equation, one soliton and an Airy-type dispersion packet (modified by the nonlinearity) are born from the delta-function, [17]. When inverting, it is obvious that large amplitudes of the rogue wave are achieved precisely by the collapse of the dispersion packet, and the soliton introduces only a small portion of energy here. If the rogue wave is not ideal, but represents a Gaussian pulse, then it scatters into a sequence of solitons, the number of which is proportional to the Ursell parameter, and the maximum amplitude of the soliton exceeds the initial amplitude, [17]. Then, when inverting, this group of solitons will focus into a Gaussian pulse, but its amplitude will be less than the amplitudes of the solitons in the group and, accordingly, this Gaussian pulse can never represent a rogue wave. Thus, though we regard a nonlinear problem, we find that the Ursell parameter of the rogue wave is small, that is, the problem might be still regarded as essentially linear. This process was studied in detail in [17], where the focusing of a dispersive packet with solitons into a rogue wave was simulated numerically. The same is valid also for modified KdV equation, where Ursell parameter of the rogue wave should be small.

• The above scenario of a rogue wave formation as a result of focusing dispersion packets and a small number of solitons (one or two) is apparently typical for the equations in which the interaction of solitons leads to their repulsion in space (as in the classical Korteweg–de Vries equation). It is closely related to the phenomenon of modulation instability, [7, 12, 29–31], or rather its absence in systems with repulsive solitons, [20, 34]. Such equations are called defocusing, and for them, in our opinion, the dispersive focusing mechanism is fundamental for the occurrence of rogue waves.

• In equations where attraction of solitons is possible, the process of modulation instability is also realized. This situation, in particular, takes place for the focusing modified Korteweg–de Vries equation which admits focusing of a large number of solitons of different polarity into a rogue wave, [32, 33]. The modulation instability of a cnoidal wave, in the extreme case (corresponding to a sequence of solitons of different polarity) also leads to the formation of a rogue wave, and this process was recently studied in [35, 36]. The processes of this type have been studied so far only in integrable systems, and it is unclear whether it is possible to proceed with these sophisticated methods to the study of non-integrable systems with solitons losing energy during interaction. On the other hand, focusing of wave packets, as follows from our analysis, takes place in both systems integrable and non-integrable and is effective for rogue waves generation.

Acknowledgments

The authors are grateful to Alexey Slunyaev for assistance in working with the MATLAB's analytical unit while deriving equation (22). ET acknowledges the support of the Austrian Science Foundation (FWF) under projects P30887 and P31163. EP is partially supported by the Laboratory of Dynamical Systems and Applications NRU HSE, of the Ministry of Science and Higher Education of the RF Grant ag. No. 075-15-2019-1931 (section 4). EP is also supported by the government research project No. 0035-2019-0007.

ORCID iDs

Elena Tobisch https://orcid.org/0000-0003-0674-6826

References

[1] Kharif C, Pelinovsky E and Slunyaev A 2009 *Rogue Waves in the Ocean* (Berlin: Springer)
[2] Ruban V *et al* 2010 Rogue waves – towards a unifying concept?: discussions and debates *Eur. Phys. J. Spec. Top.* **185** 5–15
[3] Onorato M, Resitori S, Bortolozzo U, Montina A and Arecchi F T 2013 Rogue waves and their generating mechanisms in different physical contexts *Phys. Rep.* **528** 47–89
[4] Onorato M, Resitori S and Baronio F (ed) 2016 *Rogue and Shock Waves in Nonlinear Dispersive Media* (Berlin: Springer)
[5] Dudley J M, Genty G, Mussot A, Chabchoub A and Dias F 2019 Rogue waves and analogies in optics and oceanography *Nat. Rev. Phys.* **1** 675–89
[6] Fedele F, Brennan J, Ponce de Leon S, Dudley J and Dias F 2016 Real world ocean rogue waves explained without the modulational instability *Sci. Rep.* **6** 27715
[7] Ablowitz M J 2011 *Nonlinear Dispersive Waves. Asymptotic Analysis and Solitons* (Cambridge: Cambridge University Press)
[8] Kawahara T 1972 Oscillatory solitary waves in dispersive media *J. Phys. Soc. Japan* **33** 260–4
[9] Boyd J P 1991 Weakly non-local solitons for capillary-gravity waves: fifth degree Korteweg–de Vries equation *Physica* D **48** 129–46
[10] Khusnutdinova K R, Stepanyanz J A and Tranter M R 2018 Soliton solutions to the fifth-order Korteweg–de Vries equation and their applications to surface and internal water waves *Phys. Fluids* **30** 022104
[11] Schamel H 1973 A modified Korteweg–de Vries equation for ion acoustic waves due to resonant electrons *J. Plasma Phys.* **9** 377–87
[12] Whitham G B 1999 *Linear and Nonlinear Waves* (*Series in Pure and Applied Mathematics*) (New York: Wiley)
[13] Kurkina O E, Ruvinskaya E A, Pelinovsky E N, Kurkin A A and Soomere T 2012 Dynamics of solitons in a nonintegrable version of the modified KdV equation *JETP Lett.* **95** 91–5
[14] Geyer A and Pelinovsky D E 2017 Spectral stability of periodic waves in the generalized reduced Ostrovsky equation *Lett. Math. Phys.* **107** 1293–314
[15] Wazwaz A-M 2018 Multiple complex soliton solutions for integrable negative-order KdV and integrable negative-order modified KdV equations *Appl. Math. Lett.* **88** 1–7
[16] Natali F, Le U and Pelinovsky D E 2020 New variational characterization of periodic waves in the fractional Korteweg–de Vries equation *Nonlinearity* **33** 1956–86
[17] Pelinovsky E, Talipova T and Kharif C 2000 Nonlinear dispersive mechanism of the freak wave formation in shallow water *Physica* D **147** 83–94
[18] Chabchoub A and Fink M 2014 Time-reversal generation of rogue waves *Phys. Rev. Lett.* **112** 124101
[19] Ducrozet G, Fink M and Chabchoub A 2016 Time-reversal of nonlinear waves: applicability and limitations *Phys. Rev. Fluids* **1** 054302
[20] Bronski J C, Hur V M and Johnson M A 2016 Modulational instability in equations of KdV type *New Approaches to Nonlinear Waves* (*Lecture Notes in Physics* vol 908) ed E Tobisch (Berlin: Springer)
[21] Barenblatt G I and Zel'dovich Y B 1972 Self-similar solutions as intermediate asymptotics *Annu. Rev. Fluid Mech.* **4** 285–312
[22] Matsuno Y 1980 Interaction of the Benjamin–Ono solitons *J. Phys. A: Math. Gen.* **13** 1519–36
[23] Abramovitz M and Stegun I A 1972 *Handbook of Mathematical Functions* (New York: Dover)
[24] Sidi A, Sulem C and Sulem P 1986 On the long time behavior of a generalized KdV equation *Acta Appl. Math.* **7** 35–47
[25] Saut J C 2019 Benjamin–Ono and intermediate long wave equations: modeling, IST and PDE *Nonlinear Dispersive Partial Differential Equations and Inverse Scattering. Fields Institute Communications* vol 83 ed P Miller *et al* (New York: Springer) pp 95–160

[26] Pelinovsky E N and Stepanyanz J A 1978 Linear approximation in in pulse propagation problems in nonlinear media *Radiophys. Quantum Electron.* **21** 1186–8
[27] Clarke S, Grimshaw R, Miller P, Pelinovsky E and Talipova T 2000 On the generation of solitons and breathers in the modified Korteweg–de Vries equation *Chaos* **10** 383–92
[28] Pelinovsky D E and Sulem C 1998 Bifurcations of new eigenvalues for the Benjamin–Ono equation *J. Math. Phys.* **39** 6552–72
[29] Tobisch E (ed) 2016 *New Approaches to Nonlinear Waves* (*Lecture Notes in Physics* vol 908) (Berlin: Springer)
[30] Amiranaschwili S and Tobisch E 2019 Extended criterion for the modulation instability *New J. Phys.* **21** 033029
[31] Tobisch E and Pelinovsky E 2019 Conditions for modulation instability in higher order Korteweg–de Vries equations *Appl. Math. Lett.* **88** 28–32
[32] Slunyaev A V and Pelinovsky E N 2016 The role of multiple soliton and breather interactions in generation of rogue waves: the mKdV framework *Phys. Rev. Lett.* **117** 214501
[33] Shurgalina E G and Pelinovsky E N 2016 Nonlinear dynamics of a soliton gas: modified Korteweg–de Vries equation framework *Phys. Lett.* A **380** 2049–53
[34] Bronski J C, Johnson M A and Kapitula T 2011 An index theorem for the stability of periodic traveling waves of Korteweg–de Vries type *Proc. R. Soc. Edinburgh.* A **141** 1141–73
[35] Chen J and Pelinovsky D E 2018 Rogue periodic waves in the modified Korteweg–de Vries equation *Nonlinearity* **31** 1955–80
[36] Chen J and Pelinovsky D E 2019 Periodic travelling waves of the modified KdV equation and rogue waves on the periodic background *J. Nonlinear Sci.* **29** 2797–843